Applied Catalysis B: Environmental 164 (2015) 305–315

Contents lists available at ScienceDirect

Applied Catalysis B: Environmental

journal homepage: www.elsevier.com/locate/apcatb

Ru(II) impregnated Al_2O_3, Fe_3O_4, SiO_2 and *N*-coordinate ruthenium(II) arene complexes: Multifunctional catalysts in the hydrogenation of nitroarenes and the transfer hydrogenation of aryl ketones

Serkan Dayan, Fatma Arslan, Nilgun Kalaycioglu Ozpozan*

Department of Chemistry, Faculty of Science, Erciyes University, Talas Street, 38039 Kayseri, Turkey

ARTICLE INFO

Article history:
Received 2 July 2014
Received in revised form
10 September 2014
Accepted 12 September 2014
Available online 22 September 2014

Keywords:
Transfer hydrogenation
Sulfonamide
Ruthenium
Hydrogenation of nitroarenes

ABSTRACT

Six new [RuClL(*p*-cymene)]Cl (L=N-arenesulfonyl-4,5-dichloro-o-phenylenediamines) complexes (**6–10**) were prepared from the starting complex $[RuCl_2(p\text{-}cymene)]_2$. Also, three novel Al_2O_3, Fe_3O_4, SiO_2-[RuClL(*p*-cymene)]Cl materials (**11–13**) were synthesized by an impregnation method using (**10**) and were solid-supported. The structural elucidations of the complexes and materials were characterized by different methods such as ^1H, ^{13}C-NMR, FT-IR, elemental analysis, TG/DTA, nitrogen adsorption-desorption (BET), SEM and EDX. The **6–10** complexes and **11–13** materials were applied for the transfer hydrogenation (TH) of ketones in the presence of 2-propanol (as the hydrogen source). The TH experiments showed that all complexes are average catalytic precursors (**6–10**). In particular, {[N-4-chlorobenzenesulfonyl-4,5-dichloro-o-phenylenediamine]-(*p-cymene*)-*chloro-ruthenium(II)*}*chloride* (**10**) was found to be a good catalyst in comparison to the others giving the corresponding alcohols in a good turnover frequency value of 2192 h^{-1}. Additionally, the synthesized Al_2O_3, Fe_3O_4, SiO_2-[RuClL(*p*-cymene)]Cl materials (**11–13**) obtained from the most active catalyst (**10**) were used as catalysts for the TH and their efficiency was screened in the hydrogenation of nitroarenes in aqueous media at ambient temperature in the presence of $NaBH_4$ by UV–vis spectrophotometer. Furthermore, the Fe_3O_4-[RuClL(*p*-cymene)]Cl materials can be recovered by filtration and reused for four cycles for the reduction of 2-nitroaniline. This facile and environment-friendly approach provides a green way to effectively synthesize low cost solid-supported catalysts for the reduction of nitroarenes and is promising for the development of other useful materials.

1. Introduction

The synthesis of sulfonamide ligands has attracted considerable research interest in recent times [1–4]. In particular, sulfonamides are recognized for their luminescence, molecular modeling, antimicrobial and analytical applications [5–8]. A field of increasing interest in the last few years is related to the use of homogeneous or heterogeneous catalysts in various organic reactions [9–14].

Compounds containing ruthenium are also widely used in the applications of various catalytic reactions (hydrogenation, C–H bond activation, C–N bond formation, C–C bond formation, hydrosilylation, transfer hydrogenation (TH) etc.), in biosensors, solar cells, luminescence, anti-cancer drugs, inhibition etc. In particular, ruthenium complexes/materials based on various ligands (NHC, *N*-donor, phosphine etc.) frameworks have been the focus of intense research in organometallic chemistry, in homogeneous/heterogeneous catalysis. Of these, the electronic and steric parameters of *N*-donor complexes must be modified easily. The synthesis condition of *N*-donor complexes is generally mild and does not require an argon/nitrogen atmosphere [15–26].

The transfer hydrogenation reactions of various organic molecules are necessary, typically using a hydrogen donor together with a strong base and catalyst, and are preferred for large-scale industrial applications, energy and lowering toxicity. Furthermore, the transfer hydrogenation (TH) reaction of ketones is a pivotal reaction for secondary alcohols that has recently attracted much attention [27–29]. In addition, ruthenium complexes bearing *N*-donor ligands have attracted considerable interest in the reduction of ketones as catalysts [30–35].

Likewise, ruthenium-based catalysts, especially those supported by Al_2O_3, SiO_2, TiO_2, ZnO, MWCNT, or activated carbon etc., have been prepared by various methods (such as deposition–precipitation, impregnation and co-precipitation, immobilization etc.) and used in many organic transformations

* Corresponding author. Tel.:+90 505 644 11 70; fax: +90 352 437 49 33.
E-mail address: nozpozan@erciyes.edu.tr (N. Kalaycioglu Ozpozan).

http://dx.doi.org/10.1016/j.apcatb.2014.09.025
0926-3373/

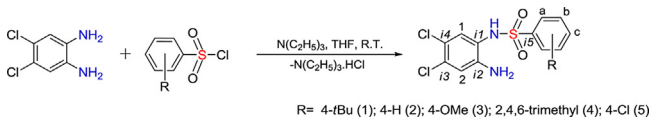

Fig. 1. Synthesis of the ligands together with NMR numbering scheme.

(reduction of nitro compounds, hydrogenation, transfer hydrogenation etc. [36–39].

Nitro compounds are a widely found organic pollutant in wastewater. Thus, the removal of the nitroarenes is an important issue. Various processes have been developed, including adsorption, photocatalysis, electrochemical treatment, the electro-Fenton method, electrocoagulation, catalytic hydrogenation etc. [40–47]. Additionally, nitroaniline derivatives have been used as precursors in the chemical synthesis of azo dyes, antioxidant compounds, poultry medicine, antiseptic agents etc. [48]. However, avoiding the use of organic solvents and the improvement of suitable processes for hydrogenation of nitroarenes in aqueous media under the mild conditions are still necessary. At the same time, some quite remarkable studies have been carried out with compounds containing ruthenium in the reduction of nitroarenes [49–51].

Herein, we chose to prepare ruthenium(II) complexes (**6–10**) prepared from *N*-arenesulfonyl-4,5-dichloro-o-phenylenediamines and then the complexes were used as catalysts in the TH of some ketones. The most effective catalyst (**10**) was supported by Al_2O_3, Fe_3O_4 and SiO2. Additionally, Al_2O_3, Fe_3O_4, SiO_2-[RuClL(*p*-cymene)]Cl materials (**11–13**) were screened for their efficiency as catalysts in the hydrogenation of nitroarenes in aqueous media at ambient temperature in the presence of $NaBH_4$ by UV–vis spectrophotometer.

2. Experimental

2.1. General procedure for the synthesis of ligands (L), **1–5**

All reagents and solvents were obtained from commercial suppliers and used without any additional purification.

The following general procedure was employed to obtain the *N-arylsulfonyl-4,5-dichloro-o-phenylenediamines:* a solution of benzenesulfonylchlorides (5 mmol) in THF (20 ml) was added drop wise over a period of 2 h into a solution of 4,5-dichloro-o-phenylenediamine (5 mmol) in the presence of triethylamine (10 mmol) in a Schlenk tube. The reaction mixture was stirred at room temperature for an additional 12 h and then filtered. Solid filtrate was left as a by-product. The volatiles were removed *in vacuo*. The residue was dissolved in DCM (15 ml) and washed with H_2O (3×20 ml) at room temperature. The organic layer was separated and dried over anhydrous $MgSO_4$, filtered, and concentrated under reduced pressure. An analytically pure sample can be isolated by recrystallization from chloroform/diethyl ether (12 ml 1:5, v/v). The desired products were dried under reduced pressure at 50 °C for 1 h. All the desired compounds were characterized by ^{1}H-NMR, ^{13}C-NMR, FT-IR and elemental analysis (Fig. 1). The NMR spectra were recorded at 297 K on a Bruker 400 NMR spectrometer at 400 MHz (^{1}H) and 100.56 MHz (^{13}C). The NMR studies were carried out in high-quality 5 mm NMR tubes. Signals are quoted in parts per million as δ downfield from tetramethylsilane (δ 0.00) as an internal standard. Coupling constants (*J*-values) are given in hertz. NMR multiplicities are abbreviated as follows: br. = broad, s = singlet, d = doublet, t = triplet, m = multiplet signal. The infrared spectra were measured with a Perkin–Elmer Spectrum 400 FTIR system and recorded using a universal ATR sampling accessory within the range 550–4000 cm^{-1}.

2.1.1. Data for the ligands **1–5**

*2.1.1.1. For N-4-tert-butylbenzenesulfonyl-4,5-dichloro-o-phenylenediamine (**1**).* Color: Light Brown. Yield: 84%. Mp: 97 °C. ^{1}H-NMR ($CDCl_3$, δ ppm): 1.34 (s, 9H, –C(CH_3)$_3$), 6.56 (s, 1H, $–H_2$), 6.78 (s, 1H, $–H_1$), 7.49 (d, 2H, *J* = 8 Hz, $–H_b$), 7.70 (d, 2H, *J* = 8 Hz, $–H_a$). ^{13}C-NMR ($CDCl_3$, ppm): 31.0 (–C(CH_3)$_3$), 35.2 (–*C*(CH_3)$_3$), 117.4 ($–C_2$H), 120.7 ($–C_1$H), 126.1 ($–C_{i3}$), 127.5 ($–C_{i4}$), 128.9 ($–C_b$H), 129.6 ($–C_a$H), 132.0 ($–C_{i1}$), 135.3 ($–C_{i5}$), 144.0 ($–C_{i2}$), 157.4 ($–C_c$). IR (cm^{-1}): 3467 and 3370 ($–NH_2$), 3225 (–NH), 3063, 3040, 2964, 2908, 2870, 1621, 1594, 1573, 1487, 1395, 1374, 1326 (ν_{as}–SO_2), 1295, 1268, 1250, 1200, 1159 (ν_s–SO_2), 1131, 1111, 1086, 1024, 1015, 971, 903, 878, 835, 784, 754, 735, 714, 679, 627, 573, 539 (**Δ**–SO_2), 521, 482, 470. Anal. Calcd. For: [$C_{16}H_{18}Cl_2N_2O_2S$] C: 51.48, H: 4.86, N: 7.50, S: 8.59. Found: C: 51.72, H: 5.02, N: 7.40, S: 8.52.

*2.1.1.2. For N-benzenesulfonyl-4,5-dichloro-o-phenylenediamine (**2**).* Color: Light Brown. Yield: 88%. Mp: 107 °C. ^{1}H-NMR ($CDCl_3$, δ ppm): 6.59 (s, 1H, $–H_2$), 6.79 (s, 1H, $–H_1$), 7.51–7.78 (m, 5H, $–H_{a-c}$). ^{13}C-NMR ($CDCl_3$, ppm): 117.6 ($–C_2$H), 120.4 ($–C_1$H), 127.5 ($–C_{i3}$), 128.9 ($–C_{i4}$), 129.1 ($–C_b$H), 129.2 ($–C_a$H), 129.7 ($–C_c$), 133.5 ($–C_{i1}$), 138.4 ($–C_{i2}$), 146.4 ($–C_{i5}$). IR (cm^{-1}): 3467 and 3374 ($–NH_2$), 3263 (–NH), 3067, 2967, 2902, 1620, 1593, 1574, 1489, 1474, 1447, 1417, 1397, 1372, 1360, 1329 (ν_{as}–SO_2), 1296, 1278, 1251, 1201, 1164 (ν_s–SO_2), 1130, 1087, 1072, 1022, 972, 913, 896, 867, 849, 817, 800, 755, 731, 710, 685, 635, 611, 583, 542 (**Δ**–SO_2), 500, 491. Anal. Calcd. For: [$C_{12}H_{10}Cl_2N_2O_2S$] C: 45.44, H: 3.18, N: 8.83, S: 10.11. Found: C: 45.88, H: 3.10, N: 8.56, S: 10.55.

*2.1.1.3. For N-4-methoxybenzenesulfonyl-4,5-dichloro-o-phenylenediamine (**3**).* Color: Light Brown. Yield: 81%. M.P.: 118 °C. ^{1}H-NMR ($CDCl_3$, δ ppm): 3.89 (s, 3H, –OCH_3), 6.63 (s, 1H, $–H_2$), 6.82 (s, 1H, $–H_1$), 6.97 (d, 2H, *J* = 8 Hz, $–H_b$), 7.71 (d, 2H, *J* = 8 Hz, $–H_a$). ^{13}C-NMR ($CDCl_3$, ppm): 56.0 (–OCH_3), 118.5 ($–C_b$H), 121.8 ($–C_2$H), 127.6 ($–C_1$H), 129.0 ($–C_{i3}$), 129.2 ($–C_{i4}$), 129.4 ($–C_a$H), 129.9 ($–C_{i1}$), 133.9 ($–C_{i5}$), 138.9 ($–C_{i2}$), 142.4 ($–C_c$). IR (cm^{-1}): 3481 and 3388 ($–NH_2$), 3279 (–NH), 2958, 2851, 1630, 1593, 1578, 1488, 1444, 1422, 1378, 1320 (ν_{as}–SO_2), 1300, 1257, 1203, 1180, 1151 (ν_s–SO_2), 1129, 1092, 1011, 973, 900, 876, 823, 801, 722, 709, 681, 666, 626, 587, 573, 555, 535 (**Δ**–SO_2), 504, 486, 472. Anal. Calcd. For: [$C_{13}H_{12}Cl_2N_2O_3S$] C: 44.97, H: 3.48, N: 8.07, S: 9.23. Found: C: 44.71, H: 3.31, N: 8.22, S: 9.01.

*2.1.1.4. For N-2,4,6-trimethylbenzenesulfonyl-4,5-dichloro-o-phenylenediamine (**4**).* Color: Light Brown. Yield: 86%. Mp: 96 °C. ^{1}H-NMR ($CDCl_3$, δ ppm): 2.32 (s, 3H, *p*-CH_3), 2.51 (s, 3H, *o*-CH_3), 6.46 (s, 1H, $–H_2$), 6.80 (s, 1H, $–H_1$), 6.96 (s, 2H, $–H_b$). ^{13}C-NMR ($CDCl_3$, ppm): 21.0 (*p*-CH_3), 23.1 (*o*-CH_3), 117.4 ($–C_2$H), 120.3 ($–C_1$H), 129.7 ($–C_{i3}$), 132.1 ($–C_{i4}$), 132.4 ($–C_b$H), 132.7 ($–C_{i1}$), 134.5 ($–C_{i5}$), 139.5 ($–C_a$), 143.2 ($–C_{i2}$), 144.5 ($–C_c$). IR (cm^{-1}): 3406 and 3367 ($–NH_2$), 3147 (–NH), 3030, 2977, 2941, 1627, 1600, 1565, 1480, 1447, 1429, 1401, 1375, 1326, 1277, 1250, 1217, 1196, 1155 (ν_s–SO_2), 1130, 1087, 1054, 1032, 1015, 965, 805, 864, 847, 816, 755, 721, 707, 675, 655, 624, 573, 527 (**Δ**–SO_2), 509, 476. Anal. Calcd. For: [$C_{15}H_{16}Cl_2N_2O_2S$] C: 50.15, H: 4.49, N: 7.80, S: 8.93. Found: C: 50.20, H: 4.39, N: 7.76, S: 8.77.

*2.1.1.5. For N-4-chlorobenzenesulfonyl-4,5-dichloro-o-phenylenediamine (**5**).* Color: Light Brown. Yield: 80%. Mp: 113 °C. ^{1}H-NMR ($CDCl_3$, δ ppm): 6.59 (s, 1H, $–H_2$), 6.77 (s, 1H, $–H_1$), 7.57 (d, 2H, *J* = 8 Hz, $–H_b$), 7.94 (d, 2H, *J* = 8 Hz, $–H_a$). ^{13}C-NMR ($CDCl_3$, ppm): 117.5 ($–C_2$H), 120.9 ($–C_1$H), 128.9 ($–C_{i3}$), 129.5 ($–C_{i4}$), 129.6 ($–C_b$H), 130.4 ($–C_a$H), 133.3 ($–C_{i1}$), 136.9 ($–C_c$), 141.5 ($–C_{i5}$), 146.2 ($–C_{i2}$). IR (cm^{-1}): 3440 and 3396 ($–NH_2$), 3252 (–NH), 3098, 3030, 2962, 1622, 1575, 1472, 1421, 1398, 1380, 1364, 1332 (ν_{as}–SO_2), 1280, 1261, 1247, 1168 (ν_s–SO_2), 1156, 1130, 1092, 1012, 968,

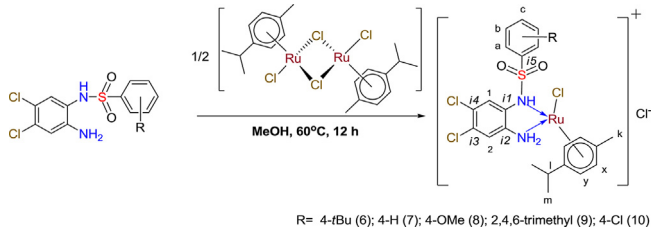

Fig. 2. Synthesis of the complexes together with NMR numbering scheme.

912, 886, 850, 824, 755, 718, 698, 679, 638, 613, 585, 546 (Δ–SO_2), 482. Anal. Calcd. For: [$C_{15}H_{16}Cl_2N_2O_2S$] C: 40.99, H: 2.58, N: 7.97, S: 9.12. Found: C: 40.82, H: 2.69, N: 7.88, S: 9.27.

2.2. General procedure for the synthesis of [Ru(p-cymene)LCl]Cl, 6–10

The synthesis of [Ru(*p-cymene*)LCl]Cl in a Schlenk flask was conducted from the reaction of **1–5** (0.50 mmol) and [$RuCl_2$(*p-cymene*)]$_2$ (0.25 mmol) in methyl alcohol (10 ml). The solution was stirred at 50 °C for 12 h. The solvent was evaporated under reduced pressure, and the residue was washed with diethyl ether (20 ml) and dried under vacuum. The desired complexes were recrystallized from MeOH to give black or dark green-colored microcrystals (Fig. 2). The [Ru(*p-cymene*)LCl]Cl type complexes were characterized by ^{1}H-NMR, ^{13}C-NMR, FT-IR, elemental analysis and conductance measurements. The synthesized ruthenium complexes are highly soluble in polar organic solvents such as chloroform, dichloromethane, DMSO and DMF and they are almost insoluble in diethyl ether and petroleum ether.

2.2.1. Data for the complexes 6–10

*2.2.1.1. For {[N-4-tert-butylbenzenesulfonyl-4,5-dichloro-o-phenylenediamine]-(p-cymene)-chloro-ruthenium(II)}chloride (**6**).* Color: Dark Green. Yield: 77%. Mp: 189 °C. ^{1}H-NMR ($CDCl_3$, δ ppm): 1.28 (d, 6H, J = 8 Hz, $-H_m$), 1.31 (s, 9H, –C(CH_3)$_3$), 2.15 (s, 3H, $-H_k$), 2.92 (m, 1H, $-H_l$), 5.36 (d, 2H, J = 4 Hz, $-H_y$), 5.50 (d, 2H, J = 4 Hz, $-H_x$), 6.48 (s, 1H, $-H_2$), 7.12 (s, 1H, $-H_1$), 7.50 (d, 2H, J = 8 Hz, $-H_b$), 7.81 (d, 2H, J = 8 Hz, $-H_a$). ^{13}C-NMR ($CDCl_3$, ppm): 18.8 (–CH_3 *(k)*), 22.2 (–CH(CH_3)$_2$), 30.7 (–C(CH_3)$_2$), 31.0 (–CH(CH_3)$_3$), 35.3 (–C(CH_3)$_3$), 80.6 ($-C_y$H), 81.3 (–CxH), 96.8, 101.3, 118.4 ($-C_2$H), 120.5 ($-C_1$H), 126.3 ($-C_{i3}$), 127.9 ($-C_{i4}$), 129.0 ($-C_b$H), 129.7 ($-C_a$H), 132.3 ($-C_{i1}$), 134.9 ($-C_{i5}$), 143.8 ($-C_{i2}$), 157.5 ($-C_c$). IR (cm^{-1}): 3323 and 3253 ($-NH_2$), 3183 (NH), 3055, 2963, 2871, 1594, 1472, 1447, 1389, 1378, 1364, 1329 (ν_{as}–SO_2), 1296, 1273, 1199, 1162 (ν_s–SO_2), 1111, 1085, 1057, 1035, 1015, 1006, 979, 877, 835, 805, 755, 734, 713, 684, 667, 655, 627, 577 (Δ–SO_2), 547, 515, 478, 455. Anal. Calcd. For: {[$C_{26}H_{32}Cl_4N_2O_2RuS$]} C: 45.96, H: 4.75, N: 4.12, S: 4.72. Found: C: 45.81, H: 4.69, N: 4.03, S: 4.61.

*2.2.1.2. For {[N-benzenesulfonyl-4,5-dichloro-o-phenylenediamine]-(p-cymene)-chloro-ruthenium(II)}chloride (**7**).* Color: Black. Yield: 79%. Mp: 194 °C. ^{1}H-NMR ($CDCl_3$, δ ppm): 1.30 (d, 6H, J = 8 Hz, $-H_m$), 2.28 (s, 6H, $-H_p$, $-H_k$), 3.06 (m, 1H, $-H_l$), 5.57 (d, 2H, J = 4 Hz, $-H_y$), 5.65 (d, 2H, J = 4 Hz, $-H_x$), 6.54 (s, 1H, $-H_2$), 7.16 (s, 1H, $-H_1$), 7.49–7.97 (m, 5H, $-H_{a-c}$). ^{13}C-NMR ($CDCl_3$, ppm): 18.5 –CH_3 *(k)*, 22.0 (–CH(CH_3)$_2$), 30.5 (–CH(CH_3)$_2$), 86.0 ($-C_y$H), 87.1 (–CxH), 97.4, 100.6, 117.1 ($-C_2$H), 120.8 ($-C_1$H), 127.4 ($-C_{i3}$), 128.9 ($-C_{i4}$), 129.2 ($-C_b$H), 129.3 ($-C_a$H), 130.7 ($-C_c$), 133.5 ($-C_{i1}$), 138.6 ($-C_{i2}$), 153.4 ($-C_{i5}$). IR (cm^{-1}): 3419 and 3352 ($-NH_2$), 3127 (–NH), 3063, 2967, 2879, 1616, 1581, 1533, 1474, 1447, 1381, 1318 (ν_{as}–SO_2), 1282, 1258, 1214, 1162 (ν_s–SO_2), 1123, 1090, 1034, 1015, 997, 961, 866, 803, 758, 727, 692, 663, 610, 574, 550 (Δ–SO_2), 534, 482. Anal. Calcd. For: {[$C_{22}H_{24}Cl_4N_2O_2RuS$]} C: 42.39, H: 3.88, N: 4.49, S: 5.14. Found: C: 42.11, H: 3.63, N: 4.50, S: 5.21.

*2.2.1.3. For {[N-4-methoxybenzenesulfonyl-4,5-dichloro-o-phenylenediamine]-(p-cymene)-chloro-ruthenium(II)}chloride (**8**).* Color: Dark Green. Yield: 74%. Mp: 188 °C. ^{1}H-NMR ($CDCl_3$, δ ppm): 1.27 (d, 6H, J = 8 Hz, $-H_m$), 2.14 (s, 3H, $-H_k$), 2.90 (m, 1H, $-H_l$), 3.83 (s, 3H, –OCH_3), 5.33 (d, 2H, J = 4 Hz, $-H_y$), 5.49 (d, 2H, J = 4 Hz, $-H_x$), 7.79 (d, 2H, J = 8 Hz, $-H_b$), 7.92 (d, 2H, J = 8 Hz, $-H_a$). ^{13}C-NMR ($CDCl_3$, ppm): 18.4–CH_3 *(k)*), 21.9 (–CH(CH_3)$_2$), 30.3 (–CH(CH_3)$_2$), 56.2 (–OCH_3), 886.0 ($-C_y$H), 87.3 (–CxH), 96.3, 101.3, 114.5 ($-C_b$H), 121.1 ($-C_2$H), 126.3 ($-C_1$H), 129.0 ($-C_{i3}$), 129.2 ($-C_{i4}$), 129.6 ($-C_a$H), 131.3 ($-C_{i1}$), 136.1 ($-C_{i5}$), 139.5 ($-C_{i2}$), 163.0 ($-C_c$). IR (cm^{-1}): 3494 and 3369 ($-NH_2$), 3152 (–NH), 3039, 2965, 2929, 2872, 1595, 1578, 1495, 1472, 1442, 1416, 1388 (ν_{as}–SO_2), 1310, 1260, 1154 (ν_s–SO_2), 1089, 1026, 966, 884, 834, 802, 707, 686, 669, 628, 585, 555 (Δ–SO_2), 494, 478, 456. Anal. Calcd. For: {[$C_{23}H_{26}Cl_4N_2O_3RuS$]} C: 42.28, H: 4.01, N: 4.29, S: 4.91. Found: C: 42.49, H: 3.92, N: 4.43, S: 4.78.

*2.2.1.4. For {[N-2,4,6-trimethylbenzenesulfonyl-4,5-dichloro-o-phenylenediamine]-(p-cymene)-chloro-ruthenium(II)}chloride (**9**).* Color: Black. Yield: 77%. Mp: 182 °C. ^{1}H-NMR (DMSO, δ ppm): 1.21 (d, 6H, J = 8 Hz, $-H_m$), 2.09 (s, 2H, $-H_k$), 2.32 (s, 3H, *p*-CH_3), 2.53 (s, 3H, *o*-CH_3), 2.81 (m, 1H, $-H_l$), 5.80 (d, 2H, J = 4 Hz, $-H_y$), 5.83 (d, 2H, J = 4 Hz, $-H_x$), 6.54 (s, 1H, $-H_2$), 7.15 (s, 1H, $-H_1$), 7.82 (d, 2H, J = 8 Hz, $-H_b$). ^{13}C-NMR (DMSO, ppm): 18.0 (–CH_3 *(k)*), 21.0 (*p*-CH_3), 23.1 (*o*-CH_3), 22.0 (–CH(CH_3)$_2$), 30.0 (–CH(CH_3)$_2$), 79.1 ($-C_y$H), 79.7 (–CxH), 93.6, 100.5, 117.2 ($-C_2$H), 120.0 ($-C_1$H), 129.8 ($-C_{i3}$), 131.7 ($-C_{i4}$), 132.9 ($-C_b$H), 133.5 ($-C_{i1}$), 136.8 ($-C_{i5}$), 139.7 ($-C_a$), 142.3 ($-C_{i2}$), 145.9 ($-C_c$). IR (cm^{-1}): 3406 and 3336 ($-NH_2$), 3147 (–NH), 3030, 2977, 2941, 1627, 1600, 1565, 1480, 1447, 1429, 1401, 1375, 1326 (ν_{as}–SO_2), 1277, 1250, 1196, 1155 (ν_s–SO_2), 1130, 1087, 1054, 1032, 1015, 965, 905, 864, 847, 816, 755, 721, 707, 675, 655, 624, 573, 527 (Δ–SO_2), 509, 476. Anal. Calcd. For: {[$C_{25}H_{30}Cl_4N_2O_2RuS$]} C: 45.12, H: 4.54, N: 4.21, S: 4.82. Found: C: 45.31, H: 4.35, N: 4.25, S: 4.97.

*2.2.1.5. For {[N-4-chlorobenzenesulfonyl-4,5-dichloro-o-phenylenediamine]-(p-cymene)-chloro-ruthenium(II)}chloride (**10**).* Color: Dark Green. Yield: 72%. Mp: 168 °C. ^{1}H-NMR ($CDCl_3$, δ ppm): 1.30 (d, 6H, J = 8 Hz, $-H_m$), 2.16 (s, 3H, $-H_k$), 2.92 (m, 1H, $-H_l$), 5.36 (d, 2H, J = 4 Hz, $-H_y$), 5.50 (d, 2H, J = 4 Hz, $-H_x$), 6.64 (s, 1H, $-H_2$), 7.13 (s, 1H, $-H_1$), 7.93 (d, 2H, J = 8 Hz, $-H_b$), 8.07 (d, 2H, J = 8 Hz, $-H_a$). ^{13}C-NMR ($CDCl_3$, ppm): 19.1 (–CH_3 *(k)*), 22.2 (–CH(CH_3)$_2$), 30.7 (–CH(CH_3)$_2$), 80.6 ($-C_y$H), 81.3 (–CxH), 96.8, 101.3, 115.9 ($-C_2$H), 119.9 ($-C_1$H), 128.5 ($-C_{i3}$), 129.6 ($-C_{i4}$), 129.7 ($-C_b$H), 130.4 ($-C_a$H), 131.4 ($-C_{i1}$), 134.7 ($-C_c$), 140.2 ($-C_{i5}$), 145.7 ($-C_{i2}$). IR (cm^{-1}): 3393 and 3324 ($-NH_2$), 3252 (NH), 3095, 2965, 2802, 1622, 1574, 1475, 1397, 1380, 1365, 1332 (ν_{as}–SO_2), 1278, 1248, 1216, 1159 (ν_s–SO_2), 1130, 1084, 1033, 1014, 966, 912, 863, 850, 823, 754, 718, 701, 679, 614, 545 (Δ–SO_2), 481. Anal. Calcd. For: {[$C_{22}H_{23}Cl_5N_2O_2RuS$]} C: 40.17, H: 3.52, N: 4.26, S: 4.87. Found: C: 40.85, H: 3.69, N: 4.43, S: 4.69.

2.3. General procedure for the transfer hydrogenation reaction

In a typical experiment, under an argon atmosphere, the ruthenium(II) complexes (0.01 mmol) and acetophenone (5 mmol) were placed in a Schlenk flask and 6 ml 2-propanol was added to the mixture, which was then stirred for 15 min at ambient temperature. Then 1 mmol base was added to the mixture and it was heated at 82 °C for the desired period of time. After the desired reaction time, the sample was diluted with diethyl ether (5 ml) and filtered from a mini-column. The purity of the compounds was checked

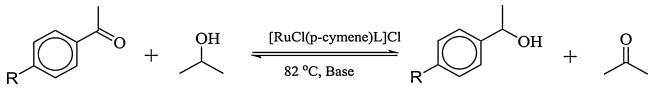

Fig. 3. Transfer hydrogenation of acetophenone derivatives with [RuCl(p-cymene)L]Cl.

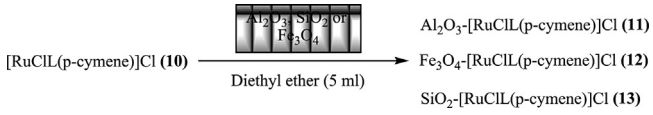

Fig. 4. The preparation of Al_2O_3, Fe_3O_4, SiO_2-supported[RuClL(*p*-cymene)]Cl, **11–13** materials.

by GC. The yields obtained were related to the residual unreacted acetophenone (Fig. 3).

GC measurements for the catalytic experiments were performed using a Younglin Acme 6100 GC instrument with a flame ionization detector and an Optima 5MS capillary column (The GC parameters were as follows: Oven: 80 °C (isothermal); Carrier gas: H_2 (Split ratio 15:1); Flow rate: 4 ml/min.; Injector port temperature: 220 °C; Detector temperature: 280 °C; Injection volume: 6.0 μl).

*2.4. General procedure for the preparation of Al_2O_3, Fe_3O_4, SiO_2-supported [RuClL(p-cymene)]Cl, **11–13***

Al_2O_3, Fe_3O_4 and SiO_2-[RuClL(*p*-cymene)]Cl materials (**11–13**) were prepared by modifying the published procedure [52].

Typically, 85 mg of >99.5% Al_2O_3, Fe_3O_4 or SiO_2 was added to 15 mg of **10** (as model complexes) in 5 ml diethyl ether (This ratio was selected randomly with the aim of setting the amount of catalyst used in each catalytic experiment). The mixture was sonicated for 1 h to form a stable suspension. After this time, the diethyl ether was then evaporated *in vacuo*. The desired pure product was dried under reduced pressure (Fig. 4).

3. Results and discussion

*3.1. Synthesis of N-(2-amino-4,5-dichlorophenyl)benzenesulfonamides (**1–5**) and their ruthenium(II) complexes (**6–10**)*

The synthesis of *N-arylsulfonyl-4,5-dichloro-o-phenylenediamines* (**1–5**) was performed in a simple one step reaction, starting from commercially available arylsulfonylchlorides and 4,5-dichloro-o-phenylenediamine (Fig. 1). In the ^{1}H-NMR spectra for sulfonamide ligands (**1–5**), the $-H_1$ and $-H_2$ protons were observed between 6.77–6.82 ppm and 6.46–6.63 ppm respectively, as a singlet. Similarly, the resonances belonging to the $-H_a$ and $-H_b$ protons were observed as a doublet and triplet, at around δ = 7.70–7.94 ppm and 6.96–7.57 ppm, respectively. In (**c**) position

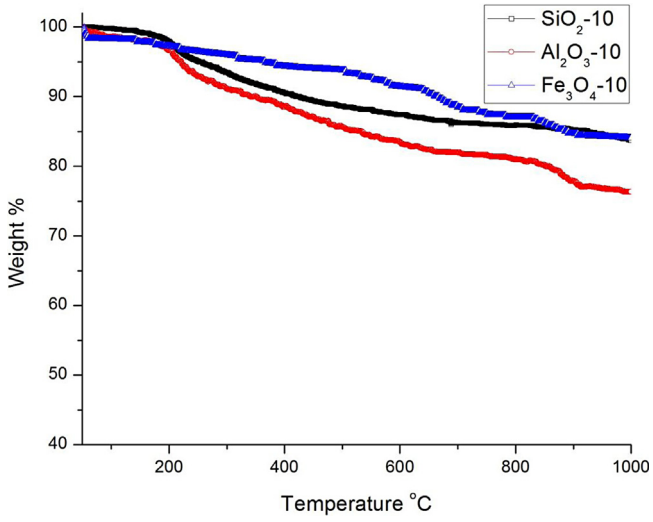

Fig. 5. TG/DTA curves of SiO_2-**10** (a), Al_2O_3-**10** (b) and Fe_3O_4-**10** (c) materials.

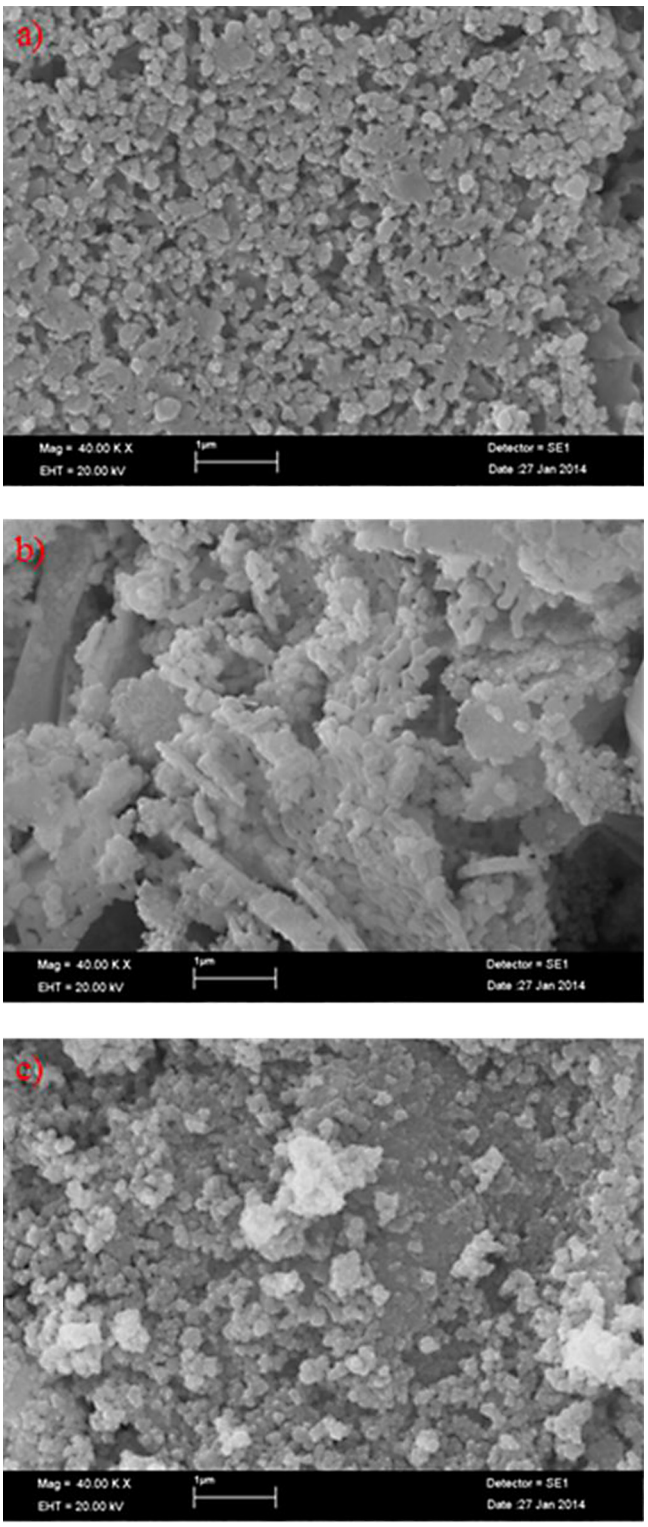

Fig. 6. SEM image of SiO_2-**10** (a), Al_2O_3-**10** (b) and Fe_3O_4-**10** (c) materials.

Table 1
TGA data of the synthesized materials (T_{on}, thermal degradation onset temperature; T_{max}, maximum weight loss temperature; T_{end}, final thermal degradation temperature).

Comp.	First degradation temp. (°C)				Second degradation temp. (°C)				Third degradation temp. (°C)				Char at 1000 °C (%)	Loss of absorbed solvent (%)
	T_{on}	T_{max}	T_{end}	Percentage of weight loss	T_{on}	T_{max}	T_{end}	Percentage of weight loss	T_{on}	T_{max}	T_{end}	Percentage of weight loss		
SiO_2-**10**	200	212	271	3.4	271	453	690	8.1	690	863	1000	0.9	85.5	2.1
Al_2O_3-**10**	132.5	204	257	5.5	257	435	790	11.55	790	883	1000	4.9	76.3	1.75
Fe_3O_4-**10**	114	248	432	4.1	432	616	737	6.1	737	884	1000	4	84	1.8

Table 2
EDX analysis data for SiO_2-**10**, Al_2O_3-**10** and Fe_3O_4-**10** materials.

Materials	Si (calc.)	Si (obs.)	Al (calc.)	Al (obs.)	Fe (calc.)	Fe (obs.)	Ru (calc.)	Ru (obs.)
SiO_2-**10**	39.73	40.02	–	–	–	–	2.304	2.351
Al_2O_3-**10**	–	–	44.99	44.82	–	–	2.304	2.278
Fe_3O_4-**10**	–	–	–	–	61.50	61.29	2.304	2.293

for **1–5**, the peaks belonging to the –*p*-CH_3, *o*-CH_3, –*p*-OCH_3 and –C(CH_3)$_3$ protons and carbons were assigned at 2.32 ppm, 2.51 ppm, 3.89 ppm and 1.34 ppm as singlets for ^{1}H-NMR and at 21.0 ppm, 23.1 ppm, 56.0 ppm, 31.0 ppm and 35.2 ppm for ^{13}C-NMR, respectively. FT-IR absorption bands belonging to the ligands were assigned at wavelengths varying from 3147 to 3481 for $\upsilon_{(NH\ or\ NH2)}$.

N-coordinated complexes were used as nucleophiles to cleave the [$RuCl_2$(p-cymene)]$_2$ dimer and the resultant *N*-coordinated ruthenium complexes (**6–10**) occurred in high yields. All complexes were isolated as dark green or black and are stable in the solid state and in solution. The structures of all complexes were confirmed by FT-IR, NMR, elemental analysis and conductance measurements. In ^{1}H-NMR the spectra for –H_k, –H_x, –H_y, –H_l and –H_m protons relating to *p*-cymene are shown as data for **6–10**. In the ^{13}C-NMR spectra for the Ru(II) complexes (**6–10**), the peaks belonging in (**c**) position, to the –*p*-CH_3, *o*-CH_3, –*p*-OCH_3 and –C(CH_3)$_3$ protons and carbons are also shown in Section 2 for **6–10**. The NMR chemical shifts and integrations of signals were consistent with the proposed structure. The representative NMR spectra are shown in Fig. S1 as supporting information. In addition, in the ruthenium complexes **6–10**, the N–H stretching frequency peaks belonging to the sulfonamide groups appeared at 3183 cm^{-1}, 3127 cm^{-1}, 3152 cm^{-1}, 3147 cm^{-1} and 3252 cm^{-1} and NH_2 stretching frequency peaks were observed at 3323–3253, 3419–3352, 3494–3369, 3406–3336 and 3393–3324 cm^{-1}, respectively. The peak frequency shifted nearly 50–200 cm^{-1} to a lower wave number which supports the participation of the –NH_2 group of these ligands in binding to the ruthenium. In addition, the formation of peaks belonging to [RuClL(*p*-cymene)]Cl are clearly seen in the FT-IR spectra of the supported materials (Fig. S3).

Concurrently, conductance measurements were also performed at ambient temperature on 1.00×10^{-3} M samples in methyl alcohol in the presence of a standard KCl solution (1.00×10^{-3} M). The molar conductance measurements were obtained as 92.5 μs for KCl, 82.6 μs for **6**, 86.7 μs for **7**, 81.5 μs for **8**, 88.9 μs for **9** and 85.4 μs for **10**.

Additionally, in Section 2, it was shown that these complexes are highly soluble in polar solvents and insoluble in diethyl ether. These solubility results are characteristic of an ionic complex. Furthermore, the synthesis of a cationic (p-cymene)Ru(II) complex bearing a chelating o-phenylenediamine group, which was prepared in a similar procedure was reported [53]. In addition, the sulfonamide group can be easily deprotonated of with amide NH [54] or vice versa [55]. These results confirmed the proposed structure.

3.2. Thermal behaviour

Thermogravimetry (TG) and differential thermal analysis (DTA) were carried out by using the DTA/TG system (Perkin Elmer Diamond type). Melting points were determined in open capillary tubes on a digital Electrothermal 9100 melting point apparatus and DTA/TG system. The thermograms of Al_2O_3, Fe_3O_4, SiO_2-supported [RuClL(*p*-cymene)]Cl materials are provided in Fig. 5. The results of the TG curves are also outlined in Table 1. In accordance with the TG curves, Al_2O_3, Fe_3O_4, SiO_2-[RuClL(*p*-cymene)]Cl materials were decomposed from organic molecules and volatiles in three steps at 50–1000 °C. Table 1 shows that SiO_2-**10**, Al_2O_3-**10** and Fe_3O_4-**10** catalysts absorbed the solvent in ratios of 2.1%, 1.75% and 1.8%, respectively.

3.3. X-ray powder diffraction analysis

Powder X-ray diffraction studies were carried out to analyze the formation of patterns. The XRD spectra demonstrated that all the Ru(II) impregnated Al_2O_3, Fe_3O_4, SiO_2 materials produced the characteristic peaks similar to those of Al_2O_3, Fe_3O_4, SiO_2 (Fig. S2 in supporting information). However, all the XRD data, in addition to the data of the pure supports (Al_2O_3, Fe_3O_4, SiO_2), have new peaks. The structure confirms the effectiveness of the simple wet impregnation method for the synthesis of Al_2O_3, Fe_3O_4, SiO_2-[RuClL(*p*-cymene)]Cl materials.

3.4. Fourier transform infrared spectroscopy for SiO_2-**10**, Al_2O_3-**10** and Fe_3O_4-**10**

The FT-IR spectra of SiO_2-**10**, Al_2O_3-**10** and Fe_3O_4-**10** are shown in Fig. S3. Herein, despite the fact that the formation of peaks belonging to **10** complex is not shown in the initial curve as supports (SiO_2, Al_2O_3, Fe_3O_4), the SiO_2, Al_2O_3 and Fe_3O_4 appears black, and the formation of peaks belonging to **10** complex is clearly seen in Fig. S3 (in supporting information) as (*). In summary it was found that, **10** complex is supported by SiO_2, Al_2O_3 and Fe_3O_4 after the impregnation method.

3.5. SEM-EDX analysis

Scanning electron microscopy (SEM) images and EDX analysis were performed on a LEO 440 model scanning electron microscope using an accelerating voltage of 20 kV.

The surface morphologies of SiO_2-**10**, Al_2O_3-**10** and Fe_3O_4-**10** materials are depicted in Fig. 6. From the SEM image, it can be

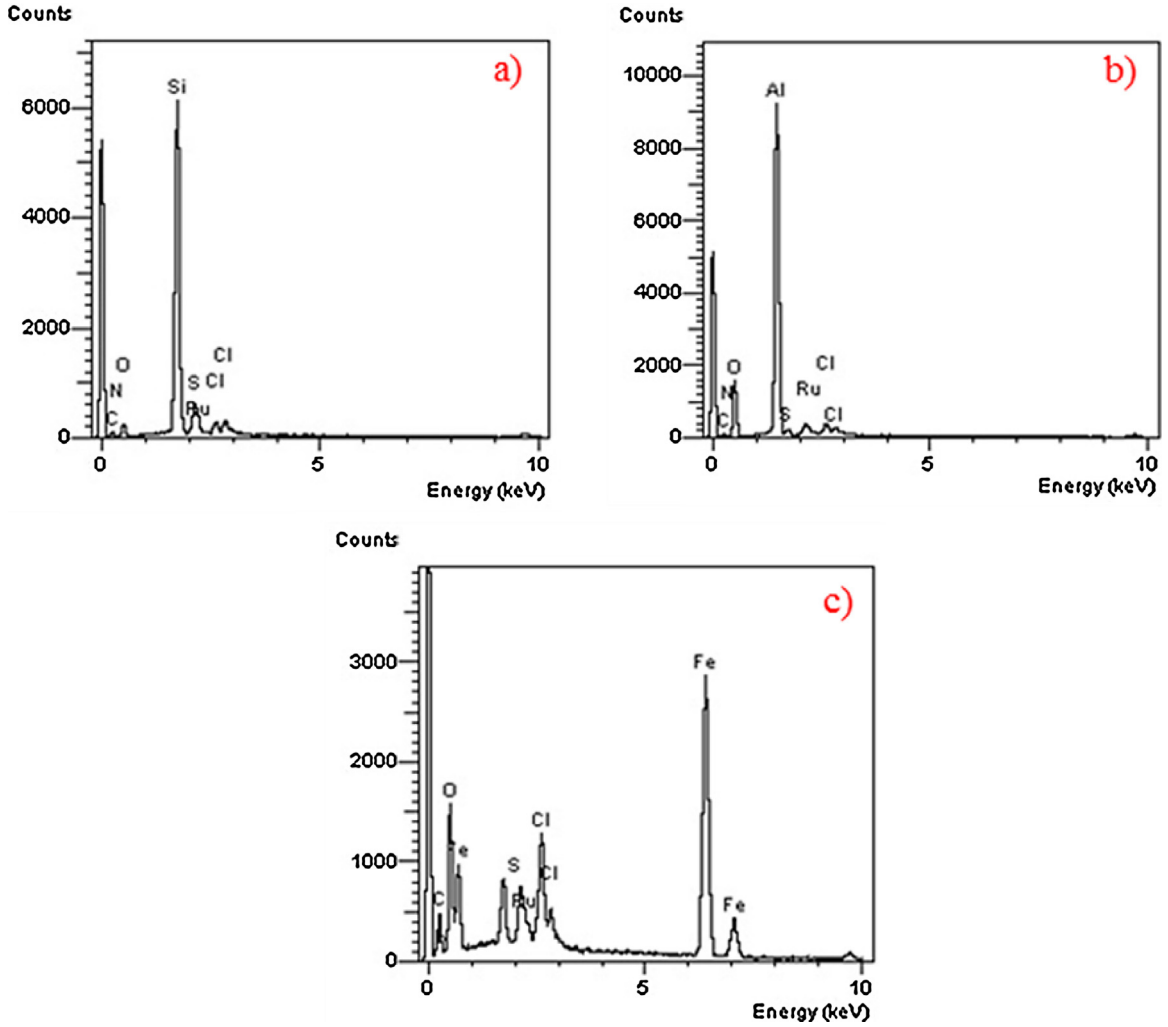

Fig. 7. EDX analysis of SiO_2-**10** (a), Al_2O_3-**10** (b) and Fe_3O_4-**10** (c) materials.

concluded that the [RuClL(*p*-cymene)]Cl (**10**) was embedded in the SiO_2, Al_2O_3 and Fe_3O_4 in powder form, respectively and it is impossible to see them from a low resolution SEM image. However, the EDX analysis image belonging to SiO_2-**10**, Al_2O_3-**10** and Fe_3O_4-**10** materials supported the structure of all the compounds. In addition, the analytic data of Si, Al, Fe and Ru are shown in Table 2. The EDX spectra given in Fig. 7(a–c) reveal that [RuClL(*p*-cymene)]Cl is supported by SiO_2, Al_2O_3, and Fe_3O_4, respectively and consists of C, N, O, S, Cl, Ru, Si, Al and Fe as expected.

3.6. N_2 adsorption–desorption isotherms

Surface area, pore volume and pore width were calculated using the nitrogen adsorption–desorption (BET) isotherm with a Micromeritics Gemini VII Surface Area and Porosity system.

The BET surface area ($m^2\,g^{-1}$), BJH pore volume ($cm^3\,g^{-1}$) and BJH pore width (nm) were calculated by the N_2 adsorption–desorption (BET) isotherms of the SiO_2-**10**, Al_2O_3-**10** and Fe_3O_4-**10** catalysts. The results indicate that the BET isotherms of Al_2O_3, Fe_3O_4, SiO_2-[RuClL(*p*-cymene)]Cl (**11**–**13**) materials were identified as typical type IV isotherms according to IUPAC (Fig. 8). The BET surface areas (S_{BET}) of SiO_2-**10**, Al_2O_3-**10** and Fe_3O_4-**10** were recorded as 248.5269 $m^2\,g^{-1}$, 9.0165 $m^2\,g^{-1}$ and 61.9064 $m^2\,g^{-1}$, respectively. The S_{BET} surface area of

Table 3
Adsorption–desorption characteristics of SiO_2-**10**, Al_2O_3-**10** and Fe_3O_4-**10** materials.

Materials	BET surface area ($m^2\,g^{-1}$)	BJH pore volume ($cm^3\,g^{-1}$)	BJH pore width (nm)
SiO_2-**10**	248.5269	0.464737	5.6702
Al_2O_3-**10**	9.0165	0.073450	27.9839
Fe_3O_4-**10**	61.9064	0.445491	22.9663

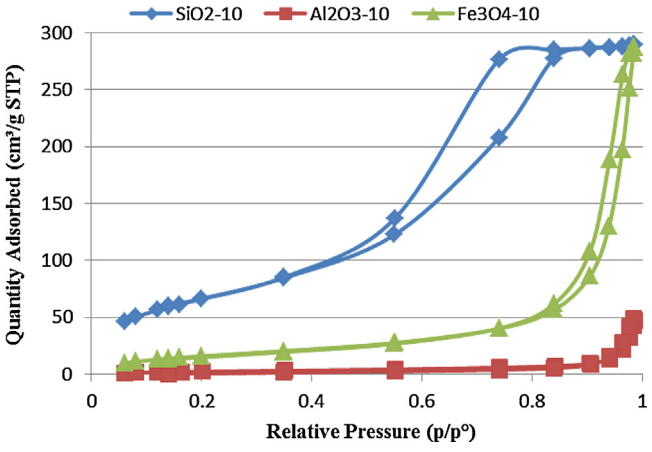

Fig. 8. BET isotherms of SiO_2-**10**, Al_2O_3-**10** and Fe_3O_4-**10**.

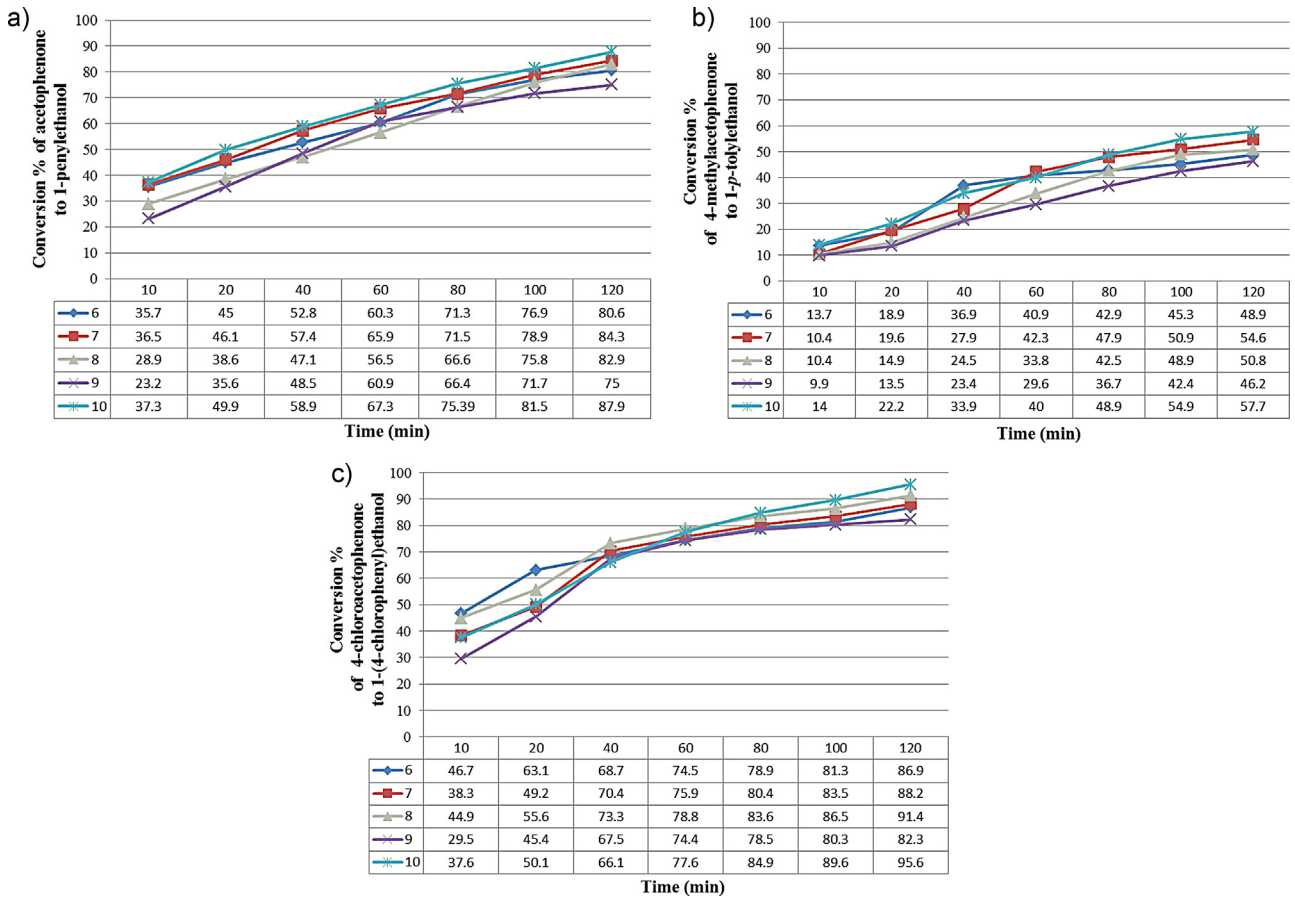

a)

	10	20	40	60	80	100	120
6	35.7	45	52.8	60.3	71.3	76.9	80.6
7	36.5	46.1	57.4	65.9	71.5	78.9	84.3
8	28.9	38.6	47.1	56.5	66.6	75.8	82.9
9	23.2	35.6	48.5	60.9	66.4	71.7	75
10	37.3	49.9	58.9	67.3	75.39	81.5	87.9

b)

	10	20	40	60	80	100	120
6	13.7	18.9	36.9	40.9	42.9	45.3	48.9
7	10.4	19.6	27.9	42.3	47.9	50.9	54.6
8	10.4	14.9	24.5	33.8	42.5	48.9	50.8
9	9.9	13.5	23.4	29.6	36.7	42.4	46.2
10	14	22.2	33.9	40	48.9	54.9	57.7

c)

	10	20	40	60	80	100	120
6	46.7	63.1	68.7	74.5	78.9	81.3	86.9
7	38.3	49.2	70.4	75.9	80.4	83.5	88.2
8	44.9	55.6	73.3	78.8	83.6	86.5	91.4
9	29.5	45.4	67.5	74.4	78.5	80.3	82.3
10	37.6	50.1	66.1	77.6	84.9	89.6	95.6

Fig. 9. Catalytic activity as shown by the % conversion vs. time for the transfer hydrogenation of (a) acetophenone, (b) 4-methylacetophenone, (c) 4-chloroacetophenone catalyzed by compounds **6–10** in 2-propanol. Conditions: p-substitued acetophenone/Ru/KOH, 5:0.01:1; T = 82 °C.

SiO_2-**10** is high compared to Al_2O_3-**10** and Fe_3O_4-**10** (Table 3). The Table 3 shows the corresponding BJH pore widths of 5.6702 nm, 27.9839 nm and 22.9663 nm, respectively.

3.7. *Ruthenium-catalysed transfer hydrogenation of acetophenone derivatives*

The ruthenium complexes were tested for the TH of p-substitute acetophenones to secondary alcohols. Initially, we investigated the influence of various bases. The base alteration experiments were carried out using an S/C = 500/1 molar ratio with model catalyst **10** and the reaction was also performed without any base but no reaction was observed even after 2 h. The addition of inorganic bases like K_2CO_3 and KOtBu showed conversion rates of 28% and 57% for 2 h, respectively (Fig. S4, in supporting information). In the event of NaOH and KOH (1 mmol) being used the conversions are 72% and 88%, respectively. Concurrently, the reaction was tried with 0.01 mmol of KOH but high conversion could not be obtained (Fig. S4, in supporting information). Among the different bases used for our studies, KOH was the best choice of base. When analyzing the results, we found that conversion was strongly dependent upon the base strength, with the stronger bases giving higher conversion K_2CO_3 < KOtBu < NaOH < KOH. Therefore, KOH was selected as the base in all subsequent studies. Concurrently, KOH was tested in the TH of acetophenone in the presence of 2-propanol using an S/B 5/1 molar ratio during 120 min and the catalytic activity was observed to be very low at 8% which is similar to Ref. [14(b)].

With these optimized conditions, the catalytic TH of p-substitute acetophenone derivatives (4-methylacetophenone and 4-chloroacetophenone) in the presence of catalysts (**6–10**) was studied in a 2-propanol/KOH medium using an S/C/B 5/0.01/1 molar ratio and a 10/0.01/1 molar ratio (Figs. 9–10). All complexes exhibited good catalytic activities for the TH of acetophenone derivatives (Figs. 9–10). In particular, the transformation of 4-chloroacetophenone is the fastest. The highest measured TOFs were **2098** h^{-1} and **2192** h^{-1} for complexes **7** and **10** in the TH of 4-chloroacetophenone at 10 min, in an S/C = 1000/1 molar ratio, respectively. Furthermore, the catalytic efficiency of the best catalyst **10** was also tested in the TH of benzophenone (diaryl) and cyclohexanone (aliphatic ketones). In the presence of benzophenone and cyclohexanone conversion rates of 75% and 84%, respectively were achieved in 2 h with catalyst **10** (Fig. 11).

In addition, Al_2O_3, Fe_3O_4, SiO_2-supported [RuClL(*p*-cymene)]Cl type materials containing the most active catalyst **10** were also used for the TH of 4-chloroacetophenone to 1-(4-chlorophenyl) ethanol in a 2-propanol/KOH medium using an S/Ru/B 5/0.01/1 molar ratio. It is well known that Fe_3O_4-supported materials are generally active in the reduction reaction [56,57]. Herein also, the catalytic activity of the materials Al_2O_3, Fe_3O_4 and SiO_2-supported [RuClL(*p*-cymene)]Cl materials decreases in the order Fe_3O_4-**10** > SiO_2-**10** > Al_2O_3-**10** (Fig. 12). Therefore, the Fe_3O_4-**10** material in the presence of electron-withdrawing groups on the sulfonamide ring was found to be the most active catalyst of all the materials examined and reached 71% conversion in 2 h. According to these results, when compared with other SiO_2-supported Ru(II) complexes, the catalytic activity of Al_2O_3, Fe_3O_4, SiO_2-supported [RuClL(*p*-cymene)]Cl in TH reaction was found to be higher even with a lower catalyst loading [52]. Respectively, the TOFs data

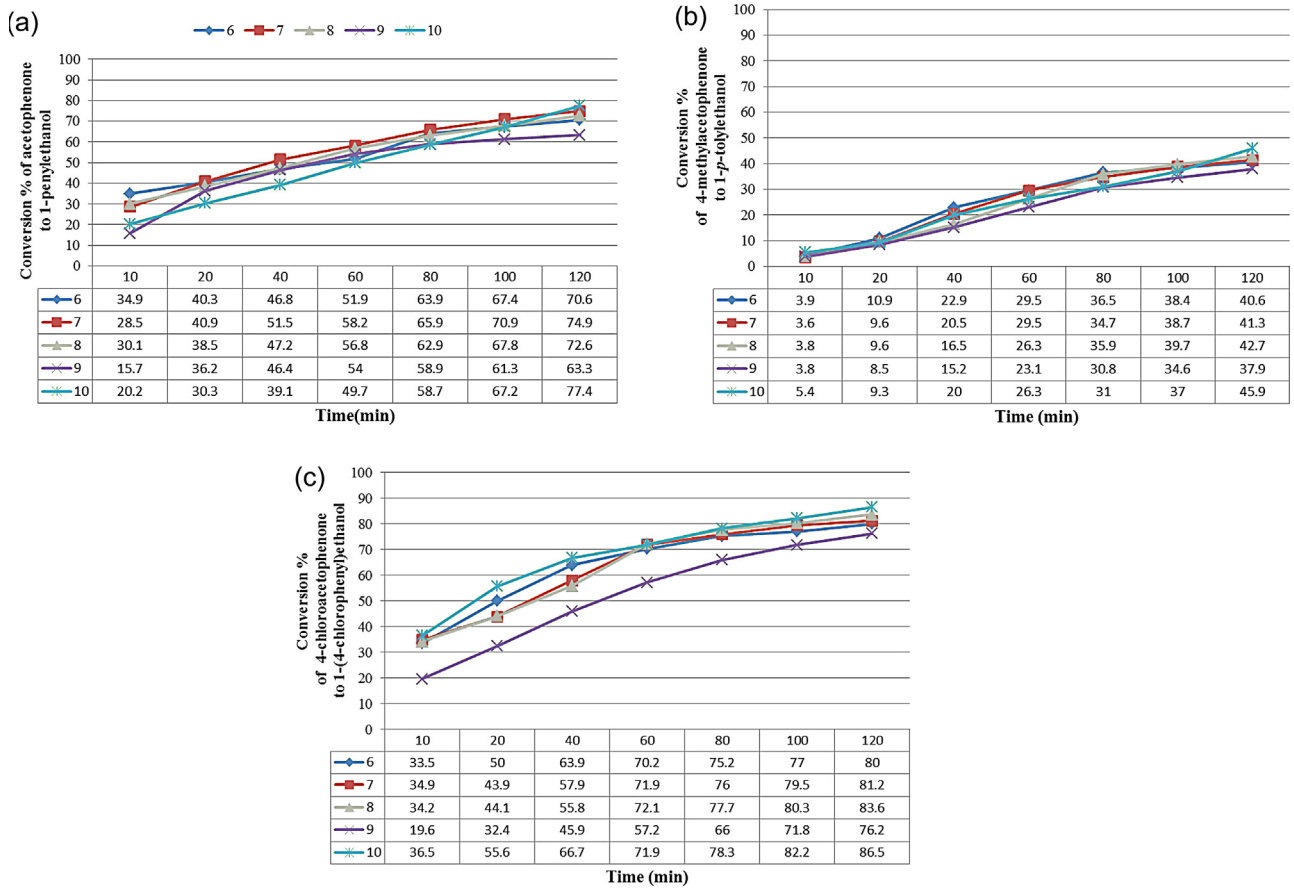

	10	20	40	60	80	100	120
6	34.9	40.3	46.8	51.9	63.9	67.4	70.6
7	28.5	40.9	51.5	58.2	65.9	70.9	74.9
8	30.1	38.5	47.2	56.8	62.9	67.8	72.6
9	15.7	36.2	46.4	54	58.9	61.3	63.3
10	20.2	30.3	39.1	49.7	58.7	67.2	77.4

	10	20	40	60	80	100	120
6	3.9	10.9	22.9	29.5	36.5	38.4	40.6
7	3.6	9.6	20.5	29.5	34.7	38.7	41.3
8	3.8	9.6	16.5	26.3	35.9	39.7	42.7
9	3.8	8.5	15.2	23.1	30.8	34.6	37.9
10	5.4	9.3	20	26.3	31	37	45.9

	10	20	40	60	80	100	120
6	33.5	50	63.9	70.2	75.2	77	80
7	34.9	43.9	57.9	71.9	76	79.5	81.2
8	34.2	44.1	55.8	72.1	77.7	80.3	83.6
9	19.6	32.4	45.9	57.2	66	71.8	76.2
10	36.5	55.6	66.7	71.9	78.3	82.2	86.5

Fig. 10. Catalytic activity as shown by the % conversion vs. time for the transfer hydrogenation of (a) acetophenone, (b) 4-methylacetophenone, (c) 4-chloroacetophenone catalyzed by compounds **6–10** in 2-propanol. Conditions: p-substituted acetophenone/Ru/KOH, 10:0.01:1; $T = 82\,^{\circ}C$.

were **390** h^{-1}, **600** h^{-1}, **450** h^{-1} for Al_2O_3, Fe_3O_4, SiO_2-supported [RuClL(*p*-cymene)]Cl in the TH of 4-chloroacetophenone at 10 min, in an S/C = 500/1 molar ratio. Concurrently, Al_2O_3, Fe_3O_4, SiO_2-supported [RuClL(*p*-cymene)]Cl type materials were also used in the reduction of nitroanilines.

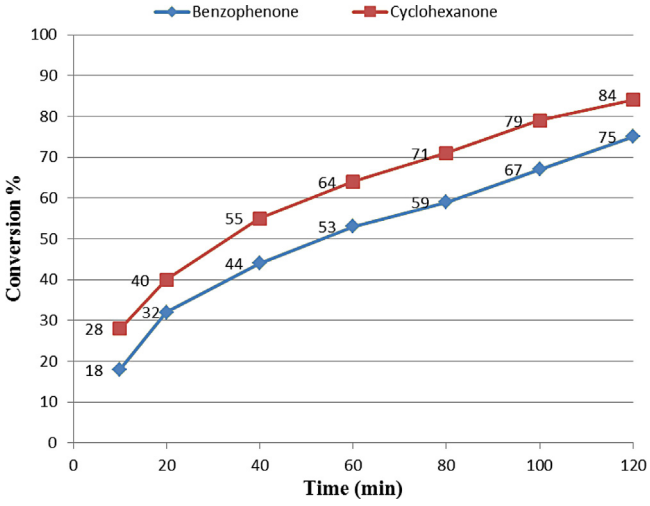

Fig. 11. Catalytic activity as shown by the % conversion vs. time for the transfer hydrogenation of benzophenone and cyclohexanone catalyzed by complex **10** in 2-propanol. Conditions: Substrate/Ru/KOH, 5:0.01:1; $T = 82\,^{\circ}C$.

3.8. Al_2O_3, Fe_3O_4, SiO_2-[RuClL(*p*-cymene)]Cl catalyzed hydrogenation of nitroanilines

The hydrogenation of nitroanilines to aminoanilines (phenylendiamines) was catalysed using $NaBH_4$ (as reducing agent) by Al_2O_3, Fe_3O_4, SiO_2-[RuClL(*p*-cymene)]Cl type catalysts (**11–13**) in aqueous medium. The hydrogenation of 2-nitroaniline, as representative substrate, was conducted to determine the optimum amount of $NaBH_4$ required for the hydrogenation of nitroanilines.

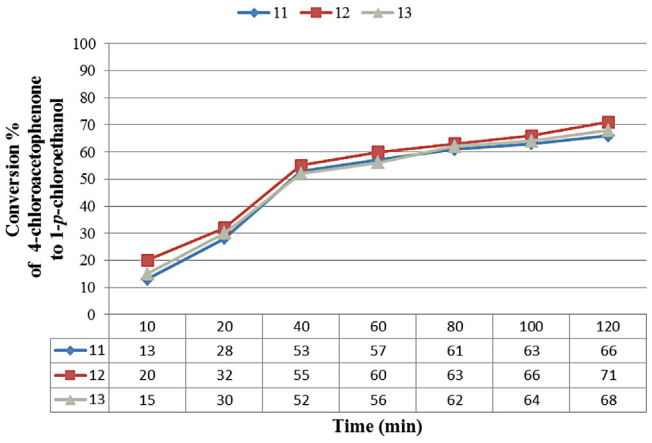

	10	20	40	60	80	100	120
11	13	28	53	57	61	63	66
12	20	32	55	60	63	66	71
13	15	30	52	56	62	64	68

Fig. 12. Catalytic activity as shown by the % conversion vs. time for the transfer hydrogenation of 4-chloroacetophenone catalyzed by compounds **11–13** in 2-propanol. Conditions: p-substituted acetophenone/Ru/KOH, 5:0.01:1; $T = 82\,^{\circ}C$.

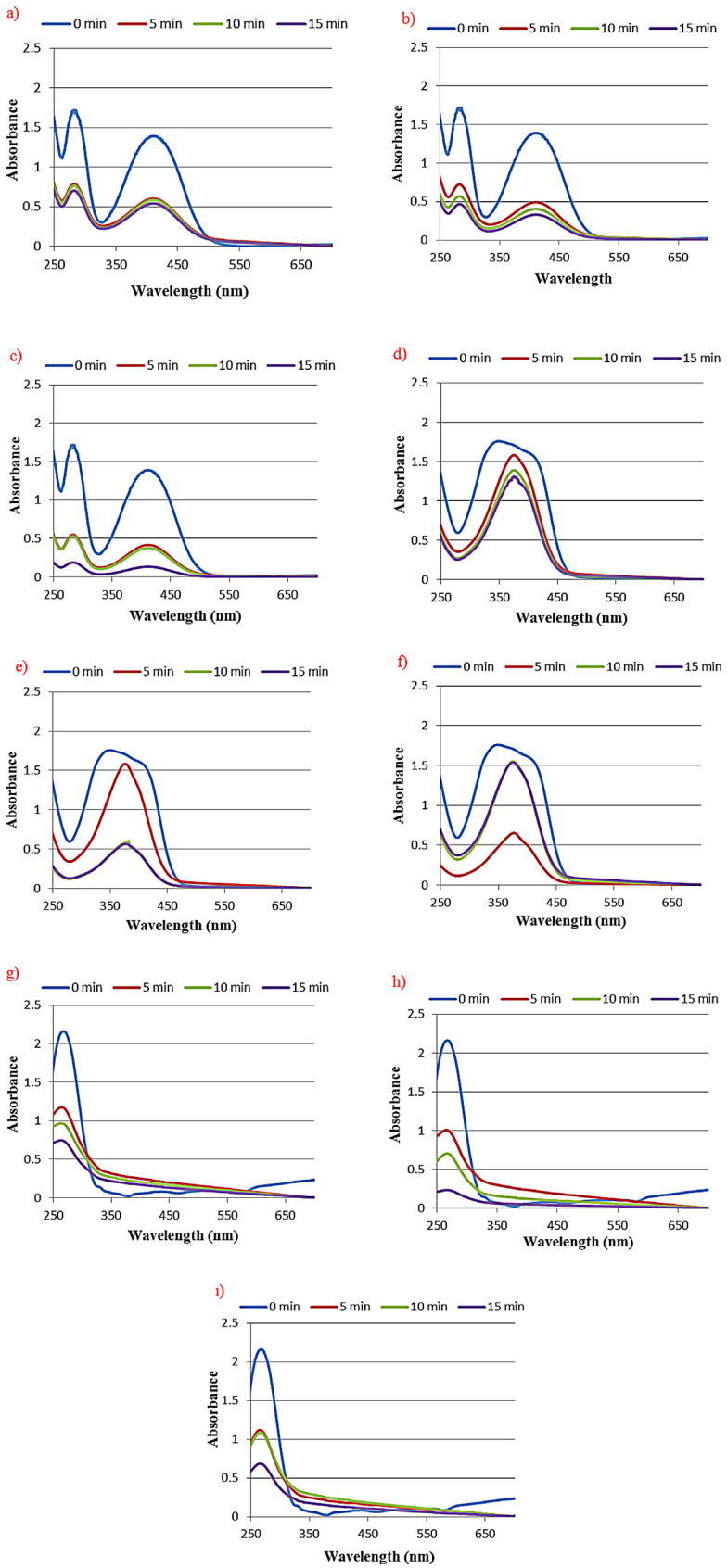

Fig. 13. Time-dependent UV–vis absorption spectra of the *o*-nitroaniline, *p*-nitroaniline and nitrobenzene reduced by $NaBH_4$ catalyzed by the (a), (d), (g) SiO_2**-10**, (b), (e), (h) Al_2O_3**-10** and (**c**), (f), (i) Fe_3O_4**-10**.

Table 4
Catalytic reduction of nitro compounds with Al_2O_3, Fe_3O_4, SiO_2-[RuClL(*p*-cymene)]Cl materials (**11–13**).

Catalyst	2-Nitroaniline		4-Nitroaniline	Nitrobenzene
	Time (min)	Conversion %[a]	Conversion %[a]	Conversion %[a]
Al_2O_3-**10**	5	64.6	7.1	53.3
	10	70.9	65.3	67.4
	15	76.2	66.7	89.2
SiO_2-**10**	5	56.8	7.5	45.4
	10	58.1	18.6	55.1
	15	61.1	24.2	65.4
Fe_3O_4-**10**	5	69.9^{I}, 61.2^{II}, 62.7^{III}, 51.4^{IV}	9.1	47.9
	10	72.7^{I}, 64.8^{II}, 65.9^{III}, 53.2^{IV}	10.2	49.5
	15	90.3^{I}, 76.3^{II}, 80.1^{III}, 58.4^{IV}	61.8	68.1

[a] % Conversion = $((A_0 - A_t)/A_0) \times 100$, A_0 is the absorbance at time ($t = 0$). A_t is value of absorbance at any time (t). I: cycle 1, II: cycle 2: III: cycle 3, IV: cycle 4.

In a model reaction, the mixture consisting of respective catalyst Fe_3O_4-**10** (**12**) (5 mg), 2-nitroaniline (2.5×10^{-4} M) and $NaBH_4$ (0.01 M) in water (10 ml) was stirred at ambient temperature for a period of 15 min. It is important that the reaction started instantly after the addition of the catalyst. The residue was monitored by ultraviolet–visible (UV–vis) spectrometry. The catalytic activities of all the materials were monitored by comparing the bands which appear and disappear after reduction on the UV–vis spectrum. UV–vis absorption measurements for the catalytic experiments were performed with Perkin-Elmer Lambda 25 UV/Vis spectrophotometers.

For the hydrogenation of 2-nitroaniline, the period of reaction was determined by measuring the change in the absorption intensity of the peak at 410 nm in the UV–vis spectrum. The characteristic band of the pure 2-nitroaniline arises at 410 nm from the $-NO_2$ group. While each reaction was realized, the UV–vis measurements were also performed at various minutes, as seen in Fig. 13. The color of the solution gradually vanished as the reaction proceeded. Additionally, there is no catalytic conversion of 2-nitroaniline in the presence of only $NaBH_4$ (0.01 M) in water (10 ml). When the Al_2O_3, Fe_3O_4, SiO_2-[RuClL(*p*-cymene)]Cl materials (**11–13**) were used as catalysts for this catalytic reaction, the catalytic effect of Al_2O_3, Fe_3O_4, SiO_2-[RuClL(*p*-cymene)]Cl increased in the order Fe_3O_4-**10** > Al_2O_3-**10** > SiO_2-**10**. As shown in Fig. 13, the reduction peak almost disappears within 15 min after the addition of Fe_3O_4-**10** to the aqueous media.

Concurrently, for the reduction of 4-nitroaniline to 4-aminoaniline (*p*-phenylendiamine), we compared the catalytic activity of Al_2O_3, Fe_3O_4, SiO_2-[RuClL(*p*-cymene)]Cl materials. Similar to 2-nitroaniline, the characteristic band of the pure 4-nitroaniline arises at 380 nm from the $-NO_2$ group. When investigating the catalytic results, those of the Al_2O_3-**10** catalyst were found to be surprisingly higher compared to the other materials (Fig. 13). Likewise, Al_2O_3, Fe_3O_4, SiO_2-[RuClL(*p*-cymene)]Cl materials were tested for the reduction of nitrobenzene to aniline under the same conditions. The band disappeared after hydrogenation at 265 nm from the $-NO_2$ group. Herein, the best catalyst was again found to be the Al_2O_3-**10** catalyst, unlike the results for the conversion of 2-nitroaniline to 2-aminoaniline. This success of the Al_2O_3-supported material is in keeping with Ref. [58,59]. On the other hand, when the position of $-NO_2$ substituent changes, such as to 2-nitroaniline, the activity of the Al_2O_3-supported material decreased compared to the Fe_3O_4-supported material. However, the reduction of the 2-nitroaniline to 2-aminoaniline (*o*-phenylendiamine) was easier than the reduction of 4-nitroaniline to 4-aminoaniline (*p*-phenylendiamine) and nitrobenzene to aniline. To ensure the reliability of the results, the catalytic reactions were repeated three times.

Therefore, the percent conversion and completion time for the hydrogenation of 2-nitroaniline, 4-nitroaniline and nitrobenzene by using Al_2O_3, Fe_3O_4, SiO_2-[RuClL(*p*-cymene)]Cl materials as catalysts are given in Table 4. The best catalyst Fe_3O_4-**10** could be recovered from the reaction mixture by filtration. As shown in Table 4, the recovered Fe_3O_4-**10** catalyst exhibited a moderate catalytic activity for at least four cycles in the reduction of 2-nitroaniline with conversion of 90.3–58.4% within 15 min.

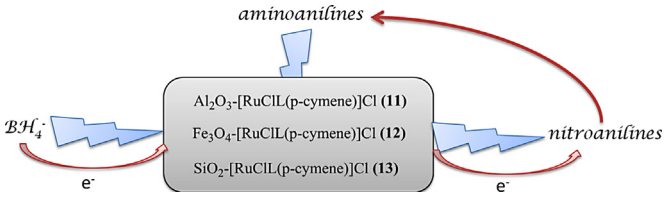

Fig. 14. Schematic representation of the reaction model of the catalytic reduction of nitroanilines (NA) to aminoanilines (phenylendiamines) (AA).

3.9. Proposed mechanism of reduction of nitroanilines with Al_2O_3, Fe_3O_4, SiO_2-supported [RuClL(*p*-cymene)]Cl

It is well known from the literature that catalytic activity is generally based on the composition of catalysts. In this context, the activity depends upon various factors like particle size, porosity, stability, the redox properties of metal ions and their distribution and electron charge potential [60]. In particularly, materials containing Ru nanoparticles, are known to be effective catalysts in the reduction of nitroanilines [61]. Herein, when Al_2O_3, Fe_3O_4, SiO_2-supported [RuClL(*p*-cymene)]Cl materials are added to the reaction media, the nitroaniline and the borohydride ions (produced by the ionization, of $NaBH_4$ in aqueous medium) diffuse from the aqueous solution towards the materials surface and around the metal ion (Ru(II)) (Fig. 14). Therefore, the metal ions present act as a medium to transfer electrons from BH_4^- to nitroaniline which leads to the formation of aminoanilines (phenylendiamines). The aqueous medium provides the H^+ ions required for the reduction of nitroanilines. The faster the electron transfers, the higher the value of the rate constant. It is evident that the catalytic reaction was fastest in the cases of Fe_3O_4-**10** and Al_2O_3-**10** as compared to SiO_2-**10**. Clearly, the presence of Fe_3O_4-supported and Al_2O_3-supported materials has a beneficial effect on the reduction reaction of nitrobenzenes. Under this reaction condition we suggest that Fe_3O_4 as support material may be preferred in the hydrogenation of 2-nitroaniline to 2-aminoaniline (o-phenylendiamine) and the Al_2O_3 support material may be usable in the formation of aminoaniline and 4-aminoaniline from nitrobenzene and 4-nitroaniline, respectively.

4. Conclusion

In summary, we have reported the fabrication and characterization of the ligands bearing sulfonamide moiety (**1–5**) and their half-sandwich Ru(II) complexes (**6–10**). Also, the activities of the

half-sandwich Ru(II) complexes were tested as catalysts in the TH of ketones in the presence of base in isopropyl alcohol (as hydrogen donor). The best catalyst **10** was also tested the ketones out of *p*-acetophenones and was found to be an as effective catalyst in the TH of benzophenone and cyclohexanone. The intriguing part of catalytic experiments is that the catalysts efficiency depends not only on the ligand but also on the substrates. Electron-withdrawing groups introduced at the *para* position of acetophenone derivatives accelerate the conversion, while the electron-donating groups slow it down. In the same way, the presence of electron-withdrawing groups on the sulfonamide ring has a beneficial effect. Generally for the complexes, the catalytic activity for the TH of ketones increases in the order **9** < **6** < **8** < **7** < **10** and the best results are found in the group of the Cl substituent for both sulfonamide ring and *p*-acetophenone. Furthermore, when benzophenone was used as substrate, a constant decrease in the catalytic conversion was observed, which was probably due to a steric effect.

In the next step, the best catalyst **10** compared to the others was selected for the impregnation methodology and was supported by the Al_2O_3, Fe_3O_4 and SiO_2. The new catalysts (**11–13**) were tested for the TH of *p*-acetophenone and reduction of nitro compounds. Interestingly, although Fe_3O_4-**10** catalyst is the best catalyst for the reduction of 2-nitroaniline, Al_2O_3-**10** catalyst is the most active for the reduction of nitrobenzene and 4-nitroaniline. Concurrently, the catalytic efficiencies for TH in the Al_2O_3, Fe_3O_4 and SiO_2-supported [RuClL(*p*-cymene)]Cl materials decrease in the order **12** (71%) > **13** (68%) > **11** (66%). Consequently, it is clear that the half-sandwich sulphonamide–Ru(II) complexes (**6–10**) used herein show moderate efficiency compared to analogues in TH reactions [62–65]. Also, the Al_2O_3, Fe_3O_4, SiO_2-supported [RuClL(*p*-cymene)]Cl materials can be proposed as good catalysts for the reduction of nitro compounds.

Appendix A. Supplementary data

Supplementary data associated with this article can be found, in the online version, at http://dx.doi.org/10.1016/j.apcatb.2014.09.025.

References

[1] M. Tabatabaee, M. Anari-Abbasnejad, N. Nozari, S. Sadegheian, M. Ghasemzadeh, Acta Crystallogr. E 63 (2007) O2099–O2100.
[2] G.E. Cami, M.E.C. Villalba, P. Colinas, G.A. Echeverria, G. Estiu, D.B. Soria, J. Mol. Struct. 1024 (2012) 110–116.
[3] J.B. Tommasino, G. Pilet, F.N.R. Renaud, G. Novitchi, V. Robert, D. Luneau, Polyhedron 37 (2012) 27–34.
[4] W.F. Wang, T. Zhang, F.J. Wang, M. Shi, Tetrahedron 67 (2011) 1523–1529.
[5] A.S. Culf, J.T. Gerig, P.G. Williams, J. Biomol. NMR 10 (1997) 293–299.
[6] S.S. Krasnikova, I.K. Yakushchenko, S.N. Shamaev, M.G. Kaplunov, Mol. Cryst. Liq. Cryst. 468 (2007) 439–445.
[7] E. Kremer, G. Facchin, E. Estevez, P. Albores, E.J. Baran, J. Ellena, M.H. Torre, J. Inorg. Biochem. 100 (2006) 1167–1175.
[8] N. Ozdemir, S. Dayan, O. Dayan, M. Dincer, N.O. Kalaycioglu, Mol. Phys. 111 (2013) 707–723.
[9] A. Szadkowska, K. Zukowska, A.E. Pazio, K. Wozniak, R. Kadyrov, K. Grela, Organometallics 30 (2011) 1130–1138.
[10] W. Jin, X.C. Li, B.S. Wan, J. Org. Chem. 76 (2011) 484–491.
[11] H.S. Zhang, R.H. Jin, H. Yao, S. Tang, J.L. Zhuang, G.H. Liu, H.X. Li, Chem. Commun. 48 (2012) 7874–7876.
[12] Y.Q. Sun, G.H. Liu, H.Y. Gu, T.Z. Huang, Y.L. Zhang, H.X. Li, Chem. Commun. 47 (2011) 2583–2585.
[13] P.N. Liu, P.M. Gu, F. Wang, Y.Q. Tu, Org. Lett. 6 (2004) 169–172.
[14] (a) S. Dayan, N.O. Kalaycioglu, Appl. Organomet. Chem. 27 (2013) 52–58; (b) S. Dayan, N. Kayaci, N.O. Kalaycioglu, O. Dayan, E.C. Ozturk, Inorg. Chim. Acta 401 (2013) 107–113.
[15] C. Janke, M.S. Duyar, M. Hoskins, R. Farrauto, Appl. Catal. B: Environ. 152–153 (2014) 184–191.
[16] J. Jae, W. Zheng, A.M. Karim, W. Guo, R.F. Lobo, D.G. Vlachos, ChemCatChem 6 (2014) 848–856.
[17] J. Li, L. Ackermann, Tetrahedron 70 (2014) 3342–3348.
[18] C. Chen, S.H. Hong, Org. Lett. 14 (2012) 2992–2995.
[19] B. Barati, M. Moghadam, A. Rahmati, V. Mirkhani, S. Tangestaninejad, I. Mohammadpoor-Baltork, J. Organomet. Chem. 724 (2013) 32–39.
[20] B. Chatterjee, C. Gunanathan, Chem. Commun. 50 (2014) 888.
[21] S. Dayan, N.O. Kalaycioglu, J.C. Daran, A. Labande, R. Poli, Eur. J. Inorg. Chem. 18 (2013) 3224–3232.
[22] S. Liu, J. Zhang, W. Tu, J. Bao, Z. Dai, Nanoscale 6 (2014) 2419–2425.
[23] K. Neuthe, F. Bittner, F. Stiemke, B. Ziem, J. Du, M. Zellner, M. Wark, T. Schubert, R. Haag, Dyes Pigments 104 (2014) 24–33.
[24] G. Tamasi, C. Bernini, G. Corbini, N.F. Owens, L. Messori, F. Scaletti, L. Massai, P.L. Giudice, R. Cini, J. Inorg. Biochem. 134 (2014) 25–35.
[25] S.S. Braga, J. Marques, E. Heister, C.V. Diogo, P.J. Oliveira, F.A.A. Paz, T.M. Santos, M. Paula, M. Marques, Biometals 27 (2014) 507–525.
[26] E. Lebon, R. Sylvain, R.E. Piau, C. Lanthony, J. Pilmé, P. Sutra, M. Boggio-Pasqua, J.L. Heully, F. Alary, A. Juris, A. Igau, Inorg. Chem. 53 (2014) 1946–1948.
[27] R. Noyori, S. Hashiguchi, Accounts Chem. Res. 30 (1997) 97–102.
[28] M.J. Palmer, M. Wills, Tetrahedron-Asymm. 10 (1999) 2045–2061.
[29] D.E.J.E. Robinson, S.D. Bull, Tetrahedron-Asymm. 14 (2003) 1407–1446.
[30] J.E.D. Martins, D.J. Morris, B. Tripathi, M. Wills, J. Organomet. Chem. 693 (2008) 3527–3532.
[31] J.E.D. Martins, G.J. Clarkson, M. Wills, Org. Lett. 11 (2009) 847–850.
[32] F.K. Cheung, A.J. Clarke, G.J. Clarkson, D.J. Fox, M.A. Graham, C.X. Lin, A.L. Criville, M. Wills, Dalton Trans. 39 (2010) 1395–1402.
[33] A.A. Mikhailine, R.H. Morris, Inorg. Chem. 49 (2010) 11039–11044.
[34] A.A. Mikhailine, M.I. Maishan, A.J. Lough, R.H. Morris, J. Am. Chem. Soc. 134 (2012) 12266–12280.
[35] J. Dimroth, U. Schedler, J. Keilitz, R. Haag, R. Schomacker, Adv. Synth. Catal. 353 (2011) 1335–1344.
[36] H. Liu, S. Liang, W. Wang, T. Jiang, B. Han, J. Mol. Catal. A: Chem. 341 (2011) 35–41.
[37] Y. Yang, Z. Weng, S. Muratsugu, N. Ishiguro, S. Ohkoshi, M. Tada, Chem. Eur. J. 18 (2012) 1142–1153.
[38] S.A. da, S. Corradini, G.G. Lenzi, M.K. Lenzi, C.M.F. Soares, O.A.A. Santos, J. Non-Cryst. Solids 354 (2008) 4865–4870.
[39] E. Castillejos, M. Jahjah, I. Favier, A. Orej, C. Pradel, E. Teuma, A.M. Masdeu-Bult, P. Serp, M. Gómeza, ChemCatChem 4 (2012) 118–122.
[40] E. Marais, T. Nyokong, J. Hazard. Mater. 152 (2008) 293–301.
[41] O.A. O'Connor, L.Y. Young, Environ. Toxicol. Chem. 8 (1989) 853–862.
[42] M.S. Dieckmann, K.A. Gray, Water Res. 30 (1996) 1169–1183.
[43] M.A. Oturan, J. Peironten, P. Chartrin, A.J. Acher, Environ. Sci. Technol. 34 (2000) 3474–3479.
[44] N. Modirsshahla, M.A. Behnajady, S. Mohammadi-Aghdam, J. Hazard. Mater. 154 (2008) 778–786.
[45] P. Canizares, C. Saez, J. Lobato, M.A. Rodrigo, Ind. Eng. Chem. Res. 43 (2004) 1944–1951.
[46] J.R. Chiou, B.H. Lai, K.C. Hsu, D.H. Chen, J. Hazard. Mater. 248-249 (2013) 394–400.
[47] F. Khan, J. Pandey, S. Vikram, D. Pal, S.S. Cameotra, J. Hazard. Mater. 254–255 (2013) 72–78.
[48] J.H. Sun, S.P. Sun, M.H. Fan, H.Q. Guo, L.P. Qiao, R.X. Sun, J. Hazard. Mater. 148 (2007) 172–177.
[49] S.G. Oh, V. Mishra, J.K. Cho, B.-J. Kim, H.S. Kim, Y.-W. Suh, H. Lee, H.S. Park, Y.J. Kim, Catal. Commun. 43 (2014) 79–83.
[50] T. Schabel, C. Belger, B. Plietker, Org. Lett. 15 (11) (2013) 2858–2861.
[51] G. Fan, W. Huang, C. Wang, Nanoscale 5 (2013) 6819–6825.
[52] S. Dayan, N.O. Kalaycioglu, O. Dayan, N. Ozdemir, M. Dincer, O. Buyukgungor, Dalton Trans. 42 (2013) 4957–4969.
[53] T. Bugarcic, A. Habtemariam, R.J. Deeth, F.P.A. Fabbiani, S. Parsons, P.J. Sadler, Inorg. Chem. 48 (2009) 9444–9453.
[54] S. Li, Q. Zhai, M. Hu, Y. Jiang, J. Coord. Chem. 62 (2009) 2709–2718.
[55] O. Soltani, M.A. Ariger, H. Vazquez-Villa, E.M. Carreira, Org. Lett. 12 (2010) 2893–2895.
[56] X. Hu, Y.-H. Deng, Z. Gao, B.-z. Liu, C. Sun, Appl. Catal. B: Environ. 127 (2012) 167–174.
[57] T. Zeng, X.-l. Zhang, H.-y. Niu, Y.-r. Ma, W.-h. Li, Y.-q. Cai, Appl. Catal. B: Environ. 134–135 (2013) 26–33.
[58] Y. Yu, X. Zhang, H. He, Appl. Catal. B: Environ. 75 (2007) 298–302.
[59] F. Cárdenas-Lizana, S. Gómez-Quero, C. Amorim, M.A. Keane, Appl. Catal. A: Gen. 473 (2014) 41–50.
[60] A. Goyal, S. Bansal, S. Singhal, Int. J. Hydrogen Energy 39 (2014) 4895–4908.
[61] P.P. Sarmah, D.K. Dutta, Green Chem. 14 (2012) 1086–1093.
[62] A. Grabulosa, A. Mannu, E. Alberico, S. Denurra, S. Gladiali, G. Muller, J. Mol. Catal. A: Chem. 363 (2012) 49–57.
[63] M.U. Raja, E. Sindhuja, R. Ramesh, Inorg. Chem. Commun 13 (2010) 1321–1324.
[64] D.J. Morris, A.M. Hayes, M. Wills, J. Org. Chem. 71 (2006) 7035–7044.
[65] P. Kumar, A.K. Singh, R. Pandey, P.Z. Li, S.K. Singh, Q. Xu, D.S. Pandey, J. Organomet. Chem. 695 (2010) 2205–2212.